Development of Usable Bevel Gearset with Length and Profile Crowning

Hermann J. Stadtfeld

Bevel Gear Technology
Chapter 2, Continued

In the previous sections, the development of conjugate bevel gearsets via hand calculations was demonstrated. The goal of this exercise was to encourage the reader to gain a basic understanding of the theory of bevel gears. This knowledge will help gear engineers to better judge bevel gear design and their manufacturing methods.

In order to make the basis of this learning experience even more realistic, this chapter will convert a conjugate bevel gearset into a gearset that is suitable in a real-world application. Length and profile crowning will be applied to the conjugate flank surfaces. Just as in the previous chapter, all computations are demonstrated as manual hand calculations. This also shows that bevel gear theory is not as complicated as commonly assumed.

— Hermann J. Stadtfeld

The conjugate bevel gearsets covered in previous sections ("Gear Mathematics for Bevel & Hypoid Gears", August 2015 *Gear Technology*, and "Development of a Face Hobbed Spiral Bevel Gearset," September/October 2015 *Gear Technology*) will not provide usable flank contact because of tolerances and load-affected deformations of the gearbox housing, the bearings and shafts, and the gear body and teeth. In addition to edge contact and load concentration, large motion transmission errors can occur that will repeat from tooth mesh to tooth mesh and cause significant operating noise. In order to design gear pairs with high load carrying capacity and low noise emission, flank crowning is required to limit the tooth contact area within the boundaries of the teeth. The art of selecting the optimal crowning is based upon satisfying two basically opposite requirements: A) the load-free or low-load operation should provide the maximal possible contact area; and B) tooth contact must not reach the boundaries of the teeth in case of high-load operation.

In low-load operation, noise emission due to tooth mesh impact is dominating. A large contact pattern and small motion transmission error keep the tooth mesh impact low and subsequently the noise at a low level. The contact pattern movement and contact zone enlargement under load require sufficient length and profile crowning in order to prevent edge contact. The most common crowning corrections used today consist of second order functions in profile and length direction. Although second order functions can only achieve a compromise between crowning requirements A and B, they are still well suited for gear pairs which are lapped after heat treatment. The reason for this is the non-linear modification due to lap removal.

In contrast to that, non-linear crowning can be applied to bevel gear pairs that are ground after heat treatment. Non-linear crowning is known under the name UMC corrections. UMC corrections can fulfill crowning requirements A and B without the usual compromises.

As an introduction to the usage of crowning and its effect on tooth contact and motion transmission error, the face hobbed Formate bevel gearset developed in the previous section will be used as a basis for a crowning development. The result is a good example of a typical bevel gearset with length and profile crowning, as is often used in the industry.

Basic gear data:

Method		continuous indexing with Gleason face hobbing
Tooth depth along face width		parallel
Shaft angle	Σ	$= 90°$
Offset	$a = TTX$	$= 0$ mm
Number of pinion teeth	z_1	$= 13$
Number of ring gear teeth	z_2	$= 35$
Outer ring gear pitch diameter	D_{02}	$= 190$ mm
Face width	$b_1 = b_2$	$= 30$ mm
Mean spiral angle	$\beta_1 = \beta_2$	$= 30°$
Pinion hand of spiral	$HOSP_1$	= left-hand
Nominal cutter radius	R_w	$= 88$ mm
Number of cutter starts	Z_w	$= 17$
Pressure angle	$\alpha_C = \alpha_D$	$= 20°$
Profile shift factor	$x = x_1 = -x_2$	$= 0$
Tooth depth factor	f_{Depth}	$= 1$
Top-root-clearance factor	f_{CL}	$= 0.2$
Profile side shift factor	$x_S = x_{S1} = -x_{S2}$	$= 0$
Pinion addendum	h_{K1}	$= (f_{Depth} + x) * m_n = 1.0 m_n$
Pinion dedendum	h_{F1}	$= (f_{Depth} + f_{CL} - x) * m_n = 1.2 m_n$
Ring gear addendum	h_{K2}	$= (f_{Depth} - x) * m_n = 1.0 m_n$
Ring gear dedendum	h_{F2}	$= (f_{Depth} + f_{CL} + x) * m_n = 1.2 m_n$

Wanted are the blade profile parameters and basic machine settings for the gear design with length and profile crowning.

Table 1 Numerical ring gear blank specifications

Ring Gear - Blank Data			
Variable	**Explanation**	**Value**	**Dimension**
z_2	number of ring gear teeth	35	-
$RINR_2$	inner cone distance (along root line)	69.56	mm
$RAUR_2$	outer cone distance (along root line)	99.56	mm
$GATR_2 = \gamma_2$	pitch angle	69.62	°
$GAKR_2$	face angle	69.62	°
$GAFR_2$	root angle	69.62	°
$ZTKR_2$	pitch apex to crossing point	0.00	mm
$ZKKR_2$	face apex to crossing point	–4.27	mm
$ZFKR_2$	root apex to crossing point	5.12	mm
$DOMR_2 = m_{f2}$	face module	4.63	mm
HGER	whole depth of teeth	8.80	mm

Table 2 Numerical pinion blank specifications

Pinion - Blank Data			
Variable	Explanation	Value	Dimension
z_1	number of teeth pinion	13	-
$RINR_1$	inner cone distance (along root line)	58.42	mm
$RAUR_1$	outer cone distance (along root line)	88.42	mm
$GATR_1 = \gamma_1$	pitch angle	20.38	°
$GAKR_1$	face angle	20.38	°
$GAFR_1$	root angle	20.38	°
$ZTKR_1$	pitch apex to crossing point	0.00	mm
$ZKKR_1$	face apex to crossing point	–11.49	mm
$ZFKR_1$	root apex to crossing point	13.78	mm
$DOMR_1 = mf_1$	face module	4.63	mm
HGER	whole depth of teeth	8.80	mm

Calculation of Blank Data

The blank data of pinion and ring gear will not change from the previous section. The required blank data — the basis for the calculations in this section — are repeated here in Tables 1 and 2.

The Creation of Length Crowning

The length curvature of a circular tooth flank is not consistent with the inverse of the cutter head radius, but is the curvature of the cone section at the reference point perpendicular to the blade pressure angle. Figure 1 shows this principle with cylinder K_1 which smooths onto the blade enveloping cone at the reference point.

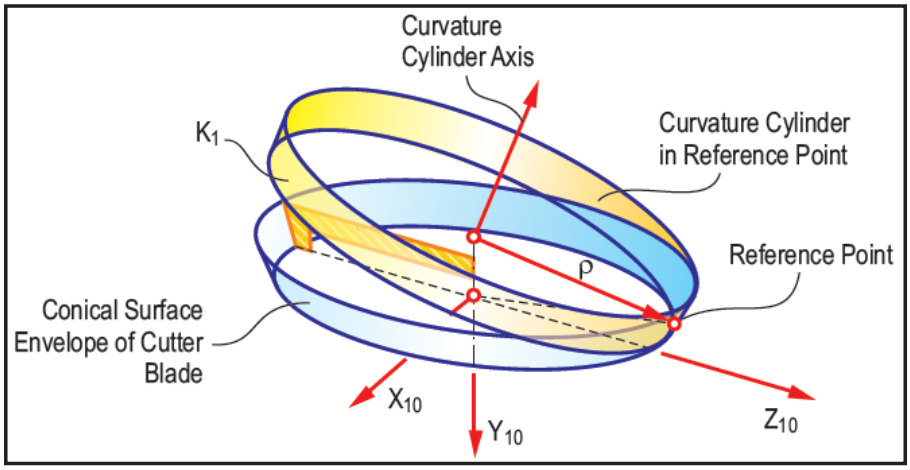

Figure 1 Blade enveloping cone and cone curvature ρ.

The tooth length curvature in Figure 1 is 1/ρ. A change in length crowning can now be realized if the axis of the cutter head is rotated (tilted) around the reference point while the cutting edge remains in the same spatial position (Fig. 2). The rotation is conducted around an axis lying in the X_4–Z_4–plane and is perpendicular to the vector R_{WOB}; i.e., R_{WIB}.

In the current example, a length crowning by tilting the ring gear cutter head should be created. First, the outside blade and the concave flank cut with it are observed (Fig. 2). If a length crowning of $\psi = 50$ µm (from center to heel and from center to toe) is desired, then the required curvature change is calculated as follows:

(1)

$$\text{The function of the crowning parabola is: } \psi = d\xi^2$$

(2)

$$\text{The second derivative of the crowning parabola is the curvature change: } \psi'' = 2d$$

With half the face width projected with the spiral angle $\beta = 30°$ onto the flank line tangent direction:

(3)

$$\xi = 15\,\text{mm} / \cos\beta = 17.32\,\text{mm}$$

and

(4)

$$\psi_{Zehe} = \psi_{Ferse} = 0.05\,\text{mm}$$

substituted in Equation 1 and solving for coefficient d delivers:

(5)

$$d = \psi / \xi^2 = 0.000167\ [1/\text{mm}]$$

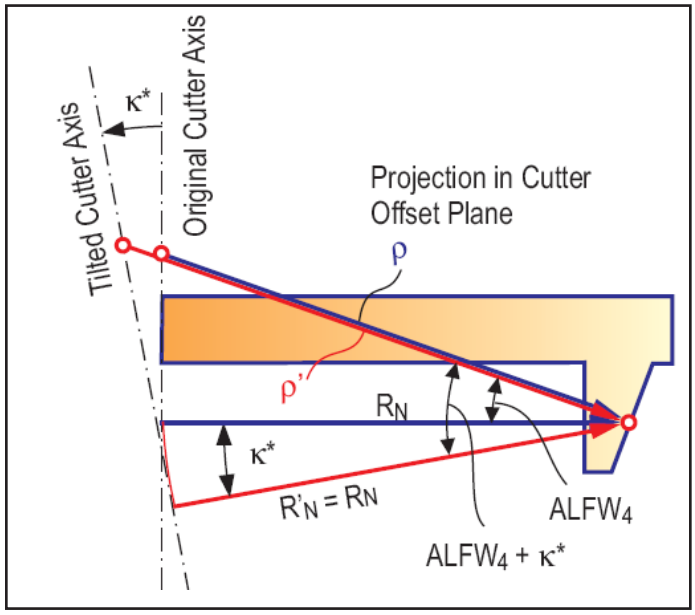

Figure 2 Cutter head tilt for generating a length crowning.

Whereas the required curvature change is:

$$\Delta K = \psi'' = 0.000333\ [1/\text{mm}] \tag{6}$$

For the creation of a positive length crowning, the curvature radius ρ of the concave flank has to increase, as shown in Figure 2. The following calculation can be derived:

From Figure 2, with $ALFW_4$ from the previous section ("Development of a Face Hobbed Spiral Bevel Gearset," September/October 2015, Eq. 4) and R_N from the previous section ("Development of a Face Hobbed Spiral Bevel Gearset," September/October 2015, Eq. 6):

$$\rho = R_N / cos\,(ALFW_{4\text{-}conjugate}) = 81.17\ /\ cos20° = 86.38\,\text{mm} \tag{7}$$

Curvature changes are added with the correct sign to the inverted curvature radii:

$$1/\rho' = 1/\rho - \Delta K \rightarrow \rho' = \rho/(1 - \Delta K_* \rho) = 88.93\,\text{mm} \tag{8}$$

Figure 2 also yields the relationship for ρ' ($R_N = R_N' = const$):

$$\rho' = R_N' / cos\,(ALFW_{4\text{-}conjugate} + \Delta\alpha) \tag{9}$$

Equation 9 can now be solved for Δα:

$$\rightarrow \Delta\alpha = arccos\,(R_N'/\rho') - ALFW_{4\text{-}conjugate} = 4.11° \tag{10}$$

The value Δα is used in order to rotate the cutter head, and with it the cutter head axis as well as the vector *RW*, around a line which lies in the X_4–Z_4–plane that is perpendicular to the vector R_{WOB}, i.e. — R_{WIB} (*see "Development of a Face Hobbed Spiral Bevel Gearset," September/October 2015, Fig. 1*). The corresponding calculations are covered in the following section.

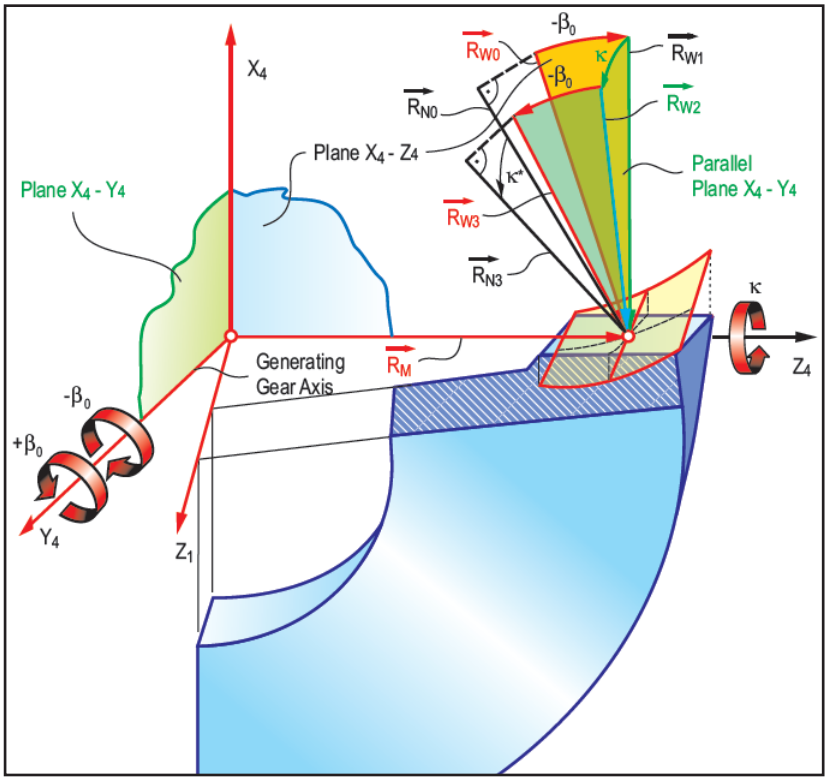

Figure 3 Rotations of normal vectors for a length crowning tilt.

Calculation of Basic Settings for the Cutting Machine

The machine settings that realize a cutter head tilt can be derived with the help of Figure 3. Vector R_{W0} lies in the generating gear plane. The first rotation around the Y_4–axis about an angle $-\beta_0$ results in vector R_{W1}. The second rotation is the real correction rotation around the Z_4–axis about an angle Δα, which results in R_{W2}. The third rotation is a back rotation into the final position (R_{W3}) about the angle $+\beta_0$ and around the Y_4–axis. β_0 is the angle of the R_W–vector in face hobbing; it is also called the "static spiral angle":

$$\beta_o = \beta - \delta_W = 7.27° \tag{11}$$

The final position differs from the starting position by a rotation Δα around the tangent of the flank line.

The rotational matrix of the negative static spiral angle $-\beta_0$ around the *Y*-axis is:

$$(-TBET) = \begin{Bmatrix} cos(-\beta_0) & 0 & sin(-\beta_0) \\ 0 & 1 & 0 \\ -sin(-\beta_0) & 0 & cos(-\beta_0) \end{Bmatrix} = \begin{Bmatrix} .9919 & 0 & -.1265 \\ 0 & 1 & 0 \\ .1265 & 0 & .9919 \end{Bmatrix} \tag{12}$$

The rotational matrix of the tilt angle Δα is:

$$(TALF) = \begin{Bmatrix} \cos\Delta\alpha & sin\,\Delta\alpha & 0 \\ -sin\,\Delta\alpha & cos\,\Delta\alpha & 0 \\ 0 & 0 & 1 \end{Bmatrix} = \begin{Bmatrix} .9974 & -.0717 & 0 \\ .0717 & .9974 & 0 \\ 0 & 0 & 1 \end{Bmatrix} \tag{13}$$

The rotational matrix of the positive static spiral angle $+\beta_0$ about the *Y*-axis is:

$$(+TBET) = \begin{Bmatrix} cos\,\beta_0 & 0 & sin\,\beta_0 \\ 0 & 1 & 0 \\ -sin\,\beta_0 & 0 & cos\,\beta_0 \end{Bmatrix} = \begin{Bmatrix} .9919 & 0 & -.1265 \\ 0 & 1 & 0 \\ .1265 & 0 & .9919 \end{Bmatrix} \tag{14}$$

The total rotation according to Figure 2 therefore yields:

$$(ROT) = (+TBET) \times (TALF) \times (-TBET) \tag{15}$$

$$(ROT) = \begin{Bmatrix} .9975 & -.0711 & .0003 \\ .0711 & .9974 & -.0091 \\ .0003 & .0091 & .9999 \end{Bmatrix} \tag{16}$$

Since the operations above are rotations versus transformations, the matrix subject to rotation is oriented at the right side of Equation 16 and is multiplied from right to left with the matrixes that include the rotations. Any number of additional rotations is possible by adding rotational matrices at the left side of the equation next to (+*TBET*).

In order to calculate the new machine settings, it is necessary to establish an actualized E_X–vector. It is evident from Figure 2 that the vector R_M remains unchanged.

$$\vec{R}_M = \{0.,\ 0.,\ 86.34\}$$
$$\vec{R}_{W0} = \{-87.29,\ 0.,\ 11.14\}$$

The new vector R_{W3} results from the multiplication of vector R_{W0} from (*text, section 2.4*) with the rotational matrix (*ROT*):

(17)

$$\vec{R}_{W3} = (\vec{ROT}) \times \vec{R}_{W0} = \begin{Bmatrix} .9975 & -.0711 & .0003 \\ .0711 & .9974 & -.0091 \\ .0003 & .0091 & .9999 \end{Bmatrix} \times \{-87.29,\ 0.,\ 11.11\}$$

(18)

$$\vec{R}_{W3} = \{-87.07,\ -6.31,\ 11.11\}$$

$$\text{This yields: } E_X = \vec{R}_M - \vec{R}_W = \{87.07,\ 6.31,\ 75.23\}$$

With the E_X–vector, the following machine settings can be calculated:

(19)

$$\text{Center roll position: } \boldsymbol{W450_{3,4}} = arctan\,(E_{XX}/E_{XZ}) = 49.17°$$

(20)

$$\text{Radial distance: } \boldsymbol{TZMM_{3,4}} = \sqrt{E_{XX}^2 + E_{XZ}^2} = 115.07\ \text{mm}$$

(21)

$$\text{Sliding base: } \boldsymbol{TYMM_{3,4}} = E_{XY} = 6.31\ \text{mm}$$

The cutter head axis Y_8 of the ring gear setup for the simple bevel gearing case in (*text section 2.4*) is collinear to the generating gear axis Y_4. Also, the axes X_8 and Z_8 have the same directions as the axes X_4 and Z_4 of the generating gear system. The orientation matrix of the cutter head coordinate system X_8–Y_8–Z_8 (cutter tilt matrix) expressed in the generating gear system is therefore a unit matrix.

(22)

$$(TKAP) = \begin{Bmatrix} 1 & 0 & 0 \\ 0 & 1 & 0 \\ 0 & 0 & 1 \end{Bmatrix}$$

The new cutter tilt matrix that accommodates length crowning is calculated by multiplication of the cutter tilt matrix (*TKAP*) with the rotational matrix (*ROT*), which includes all the necessary rotations. Since this operation is also a rotation, not a transformation, the matrix to be rotated is placed at the right end of the equation and is multiplied from right to left with the matrix that includes the rotations:

(23)

$$(TKAP_{Tilt}) = (ROT) \times (TKAP)$$

(24)

$$(ROT) = \begin{Bmatrix} .9975 & -.0711 & .0003 \\ .0711 & .9974 & -.0091 \\ .0003 & .0091 & .9999 \end{Bmatrix}$$

The mean column vector of the cutter head coordinate system matrix includes the three dimensional information of the cutter tilt. Cutter tilt and tilt orientation are calculated as follows:

(25)

$$\boldsymbol{WXMM_{3,4}} = arccos\{TKAP(2,2)\} = 4.13°$$

(26)

$$\boldsymbol{WYMM_{3,4}} = -W450_{3,4} + arctan\{TKAP(1,2)\ /\ TKAP(3,2)\} = 131.88°$$

All other machine settings remain the same. This yields the machine settings in Table 3:

Table 3 Geometrical and kinematical machine settings

Machine Basic Settings			
Variable	**Explanation**	**Value**	**Dimension**
$WXMM_{1,2}$	cutter head tilt pinion	20.38	°
$WXMM_{3,4}$	cutter head tilt ring gear	4.13	°
$WYMM_{1,2}$	swivel angle pinion	51.07	°
$WYMM_{3,4}$	swivel angle ring gear	131.88	°
$W450_{1,2}$	center roll position pinion	–51.07	°
$W450_{3,4}$	center roll position ring gear	49.17	°
$TYMM_{1,2}$	sliding base position pinion	–26.19	mm
$TYMM_{3,4}$	sliding base position ring gear	6.31	mm
$TZMM_{1,2}$	radial distance pinion	112.20	mm
TZMM34	radial distance ring gear	115.07	mm
$AWIM_{1,2}$	machine root angle pinion	–90.00	°
$AWIM_{3,4}$	machine root angle ring gear	–159.62	°
$TX2M_{1,2}$	pinion offset in the machine	0.00	mm
$TX2M_{3,4}$	ring gear offset in the machine	0.00	mm
$TZ2M_{1,2}$	machine center to crossing point pinion	0.00	mm
$TZ2M_{3,4}$	machine center to crossing point gear	0.00	mm
$UTEI_{1,2}$	indexing ratio of pinion cutting	0.764706	-
$UTEI_{3,4}$	indexing ratio of ring gear cutting	2.058824	-
$UDIF_{1,2}$	ratio of roll for pinion cutting	0.371428	-
$UDIF_{3,4}$	ratio of roll for ring gear cutting	1.000000	-

Calculation of the Cutter Head Geometry

The blade geometry of the ring gear cutter head will change as a result of the modified blade angles with constant remaining radius R_W. The amount the blade protudes beyond the generating plane remains identical to the values from the previous section ("Development of a Face Hobbed Spiral Bevel Gearset," September/October 2015, Fig. 2). This is, in case of length crowning tilt, only a compromise. In order to optimize the root fillet and avoid a step between the track of the inside blade and the outside blade, a blade stepping can be calculated. However, it is not a subject which will be covered in this example calculation.

$$\boldsymbol{S890_3} = h_{F2} = 4.80\ \text{mm}$$
$$\boldsymbol{S890_4} = h_{F2} = 4.80\ \text{mm}$$

The lead value of the cutter head tilt is the value about which the vector R_W must be rotated. This lead value has already been calculated as Δα in the previous section. The entire angle Δα is not applicable to the blade cutting edge because the cutter head normal radius vector R_N is oriented under the blade offset angle δ_W to the cutter head radius vector R_W. Vector R_N is bound to vector R_W (Fig. 3) and follows all three rotations conducted by R_W. This can be realized rather easily by the multiplication of R_N with the rotational matrix (*ROT*):

(27)

$$\vec{R}_{N0} = \{-70.295,\ 0.,\ 40.585\}$$
$$\vec{R}_{N3} = (ROT) \times \vec{R}_{N0} = \{-70.10,\ -5.37,\ 40.56\}$$

The angle between the vector R_{N0} (before the rotation) and R_{N3} (after the rotation) is derived from the scalar product between the two vectors. This angle κ* corresponds to the blade correction angle; there is only a slight difference between Δα, i.e. κ:

(28)

$$\vec{R}_{N0} \bullet \vec{R}_{N3} = \{-70.295, 0., 40.585\}\{-70.104, -5.365, 40.561\}$$
$$\vec{R}_{N0} \bullet \vec{R}_{N3} = 6574.128$$

(29)

$$|RN0| = |RN3| = RN = 81.17$$
$$\kappa^* = arccos\{(\vec{R}_{N3} \bullet \vec{R}_{N0}) / R_N^2\} = 3.794°$$

In order to cut the correct pressure angles on the ring gear

flank surfaces, new blade angles need to be calculated:

$$\boldsymbol{ALFW_4} = ALFW_{4\text{-}conjugate} + \kappa^* = 23.794° \quad (30)$$

The cutting process is considered a completing method because outside blades and inside blades are connected to the same cutter head. This means both flanks of one slot are machined at the same time. Subsequently, the length crowning by cutter head tilt can only be produced on both flanks (convex and concave) at the same time. An increase of the outside blade angle by cutter head tilt requires an equally large reduction of the inside blade angle in order to keep the gear pressure angles constant. This also leads to both flank sides having nearly identical length crowning values.

$$\boldsymbol{ALFW_3} = ALFW_{3\text{-}conjugate} - \kappa^* = 16.206° \quad (31)$$

With: $SPLF = 0$, and $R_N = 81.17$ mm, the normal blade point radii, recalculated with (*see text*) Equations 2.65 and 2.66 are:

$$\boldsymbol{RCOW_3} = R_N - SPLF/4 + h_{F2} \cdot tanALFW_3 = 82.57\,\text{mm}$$
$$\boldsymbol{RCOW_4} = R_N + SPLF/4 - h_{F2} \cdot tanALFW_4 = 79.05\,\text{mm}$$

The new cutter head and blade geometry data are recorded in Table 3.

Simulation of the Gear Cutting Process and Tooth Contact Analysis of the Example with Length Crowning

Input of the modified blade data and machine settings into the basic machine dataset for the flank generation and roll simulation program yield the analysis results in Figure 4. Already the introduction of pure length crowning leads to fundamentally different analysis results. The Ease-Off topography shows a circular material removal along the face width. The ordinate values at heel and toe of the coast side (equal to the concave ring gear flank) correspond at mid profile exactly to the 50µm which the calculation was based on. The Ease-Off topographies of coast and drive side show clear twistings. This is typical for face hobbed bevel gear sets and shows that the cutter head tilt causes differences in the epicycloids between top and root of the tooth. In the event of undesirable flank twist, which will cause a slight increase of the contact pattern bias direction, a split of the length crowning into a pinion component and a gear component can prevent a twisted Ease-Off. The split of the length crowning into pinion and gear cutting creates distortions of the epicycloids, which between pinion and gear will cancel each other out.

The motion error characteristic in Figure 4 shows very small amplitude values because the path of contact direction is mainly oriented in the profile direction. The contact patterns in the lower portion of Figure 4 are limited in face width direction, as expected. The mean points (stars in the graphics) are located at the top limitation of the active common flank area on the coast side, and at the root limitation on the drive side. The reason for this is the missing profile crowning, which causes an indifferent mean point position in profile that is influenced merely by Ease-Off changes in the single µm range. The introduction of profile crowning as demonstrated in the next section will resolve this problem.

The Creation of Profile Crowning

Ease-Off perpendicular to the tooth length direction is called profile crowning. This crowning is oriented perpendicular to the pitch line, i.e. — to the root line (depending on the process). Profile crowning is mostly achieved with blade modifications. Instead of a straight cutting edge, a curved profile is applied which is tangential to the blade pressure angle at the reference point. As an example, the development with length crowning is used. Since the initial blade profile is a straight line, the cutting edge parameters for a chosen profile crowning of $\psi = 10$ µm can be calculated with the following sequence of Equations 32 – 41:

With half of the profile depth projected about the pressure angle of $\alpha = 20°$:

$$\xi = 4\,\text{mm} / cos\alpha = 4.25\,\text{mm} \quad (32)$$

and

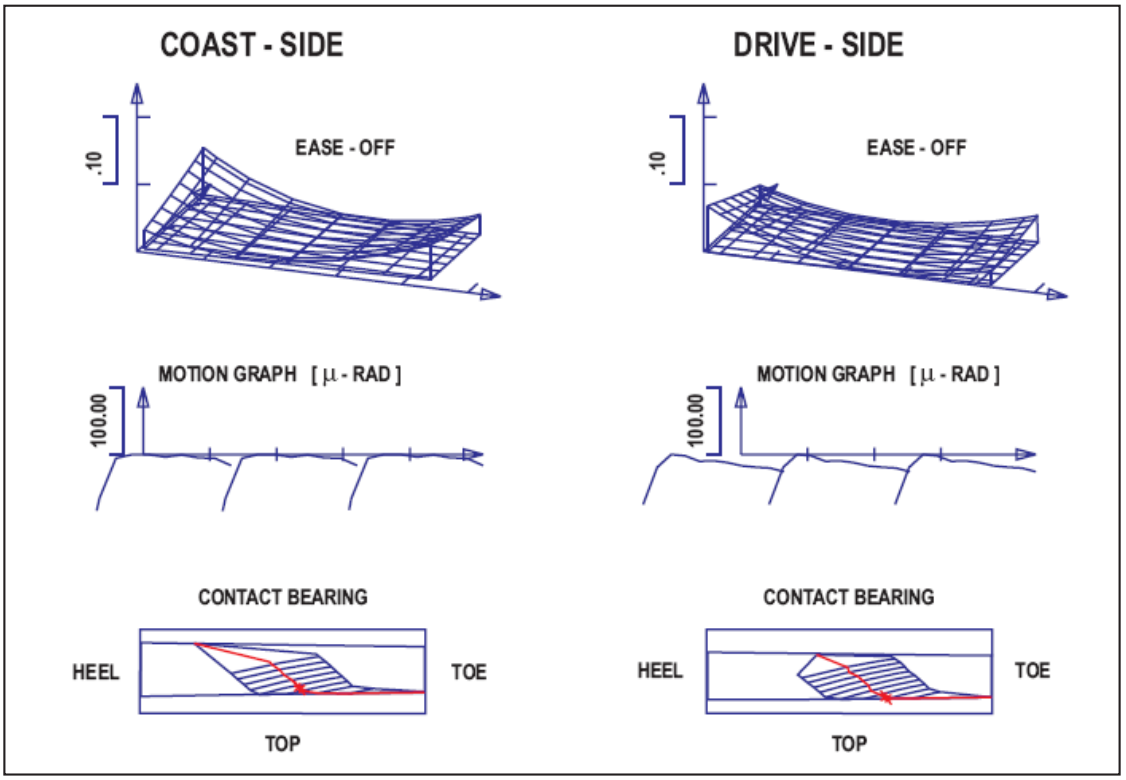

Figure 4 Graphical results of roll simulation of a pair with length crowning.

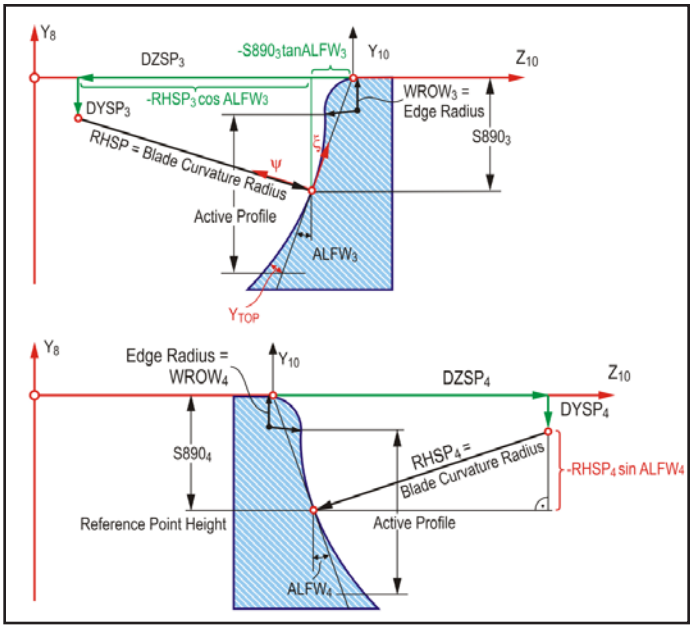

Figure 5 Blade profiles with circular correction.

$$\psi_{Top} = \psi_{Root} = 0.01\,\text{mm} \tag{33}$$

substituted into Equation 1 and solved for coefficient d results in:

$$d = \psi/\xi^2 = 0.000554 \tag{34}$$

Which gives the required curvature change with $y'' = 2d$:

$$\rho = 1 / \psi'' = 903.13\,\text{mm} \tag{35}$$

The curvature radius ρ must be applied to the blade profiles of inside and outside blades, as shown in Figure 5, in order to create positive profile crowning. The blade curvature radius *RHSP* equals ρ. All bold-printed variables are required for a complete definition of the curved blade profile:

Table 4 Cutter head and blade specifications

Cutter Head and Blade Data			
Variable	Explanation	Value	Dimension
$S890_{1,2}$	reference point to blade tip pinion	4.80	mm
$S890_{3,4}$	reference point to blade tip gear	4.80	mm
$WAME_1$	blade phase angle pinion convex	10.59	°
$WAME_2$	blade phase angle pinion concave	0.00	°
$WAME_3$	blade phase angle ring gear convex	–10.59	°
$WAME_4$	blade phase angle ring gear concave	0.00	°
$XSME_{1,2}$	blade offset in pinion cutter head	34.00	mm
$XSME_{3,4}$	blade offset in ring gear cutter head	–34.00	mm
$RCOW_1$	cutter point radius pinion inside blade	82.92	mm
$RCOW_2$	cutter point radius pinion outside blade	79.42	mm
$RCOW_3$	cutter point radius ring gear inside blade	82.57	mm
$RCOW_4$	cutter point radius ring gear outside blade	79.05	mm
$ALFW_1$	blade angle pinion inside blade	20.00	°
$ALFW_2$	blade angle pinion outside blade	20.00	°
$ALFW_3$	blade angle ring gear inside blade	16.21	°
$ALFW_4$	blade angle ring gear outside blade	23.79	°

$$\boldsymbol{RHSP}_3 = \rho = 903.13\,\text{mm} \tag{36}$$

$$\boldsymbol{DYSP}_3 = S890_3 - RHSP_3 sin\,(ALFW_3) = -242.47\,\text{mm} \tag{37}$$

$$\boldsymbol{DZSP}_3 = -RHSP_3 cos\,(ALFW_3) - S890_3 tan\,(ALFW_3) = -869.99\,\text{mm} \tag{38}$$

$$\boldsymbol{RHSP}_4 = \rho = 903.13\,\text{mm} \tag{39}$$

$$\boldsymbol{DYSP}_4 = S890_4 - RHSP_4 sin\,(ALFW_4) = -364.12\,\text{mm} \tag{40}$$

$$\boldsymbol{DZSP}_4 = RHSP_4 cos\,(ALFW_4) + S890_4 tan\,(ALFW_4) = 826.49\,\text{mm} \tag{41}$$

This leads to cutter head and blade geometry according to the data in Table 4. Only the ring gear blade data, with reference to the definition of the curved cutting edges, are added to the values in Table 3.

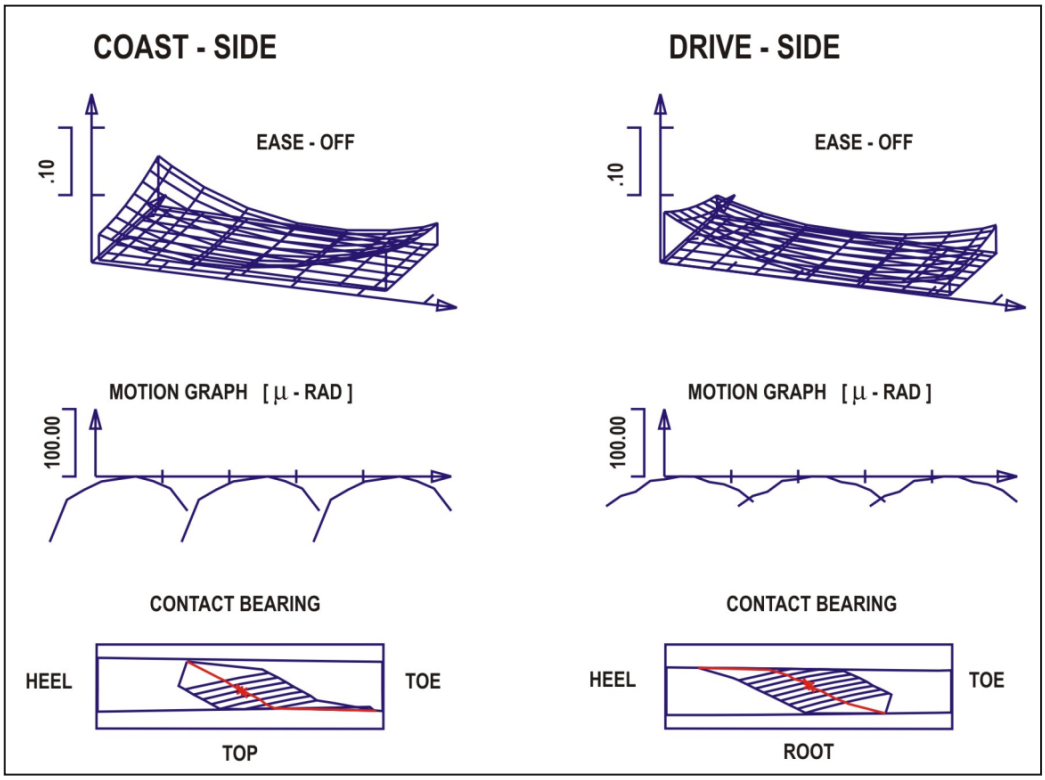

Figure 6 Graphical results of roll simulation (TCA) of a pair with length and profile crowning.

Simulation of the Gear Cutting Process and Tooth Contact Analysis of the Example with Length and Profile Crowning

After inputing the blank data from Tables 1 and 2, the modified machine settings from Table 2 and the blade data from Table 4 for creating length and profile crowning into the basic machine dataset of the flank generation and roll simulation program, the analysis results in Figure 6 are acquired.

The Ease-Off topographies for coast and drive side in Figure 6 now have a circular curve in length as well as in profile direction. This Ease-Off makes the gear design insensitive to manufacturing tolerances and load affected deformations. The motion transmission error in the middle of the figure shows a parabola-shape graph for each of the three preceding pairs of teeth.

The tooth contact pattern in the lower part of Figure 6 shows a bias in characteristic — typical for bevel gear pairs manufactured in the face hobbing process. The mean points (stars at the contact center) are now centered at the middle of the profile. The results of this section not only show a usable, but a well-designed, typical bevel gearset as it is developed for hard finishing by lapping. Small deficiencies in the amount of active profile can be eliminated with a profile shift.

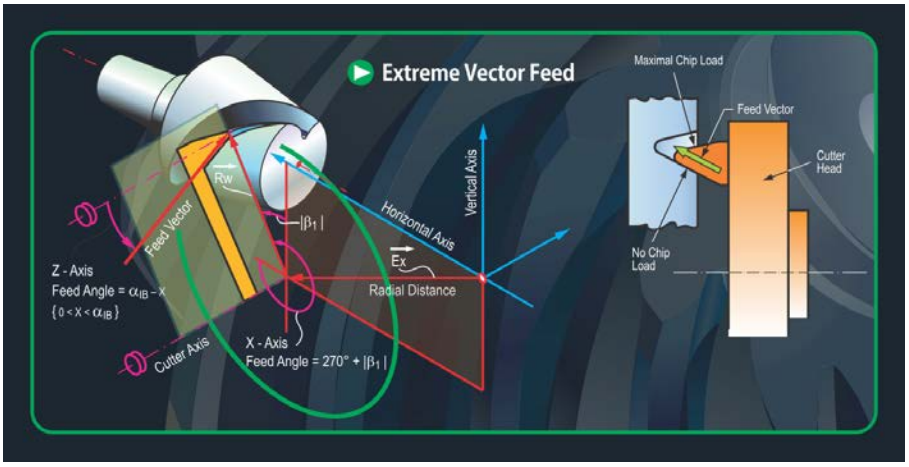

Figure 7 Extreme vector feed of a tilted cutter.

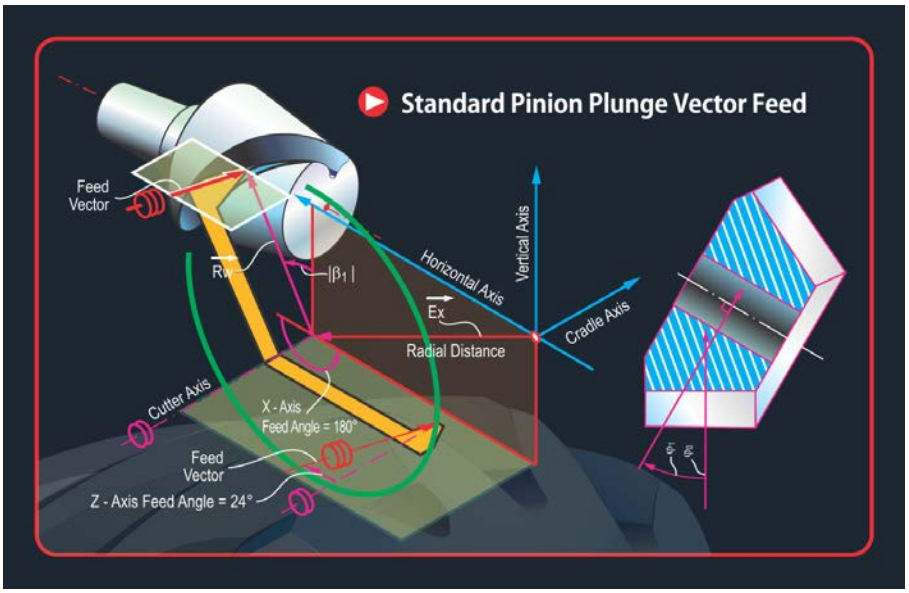

Figure 8 Pinion vector feed of a tilted cutter 180 – 24."

For Related Articles Search
bevel gears
at www.geartechnology.com

Dr. Hermann J. Stadtfeld received in 1978 his B.S. and in 1982 his M.S. degrees in mechanical engineering at the Technical University in Aachen, Germany; upon receiving his Doctorate, he remained as a research scientist at the University's Machine Tool Laboratory. In 1987, he accepted the position of head of engineering and R&D of the Bevel Gear Machine Tool Division of Oerlikon Buehrle AG in Zurich and, in 1992, returned to academia as visiting professor at the Rochester Institute of Technology. Dr. Stadtfeld returned to the commercial workplace in 1994 — joining The Gleason Works — also in Rochester — first as director of R&D, and, in 1996, as vice president R&D. During a three-year hiatus (2002–2005) from Gleason, he established a gear research company in Germany while simultaneously accepting a professorship to teach gear technology courses at the University of Ilmenau. Stadtfeld subsequently returned to the Gleason Corporation in 2005, where he currently holds the position of vice president, bevel gear technology and R&D. A prolific author (and frequent contributor to Gear Technology), Dr. Stadtfeld has published more than 200 technical papers and 10 books on bevel gear technology; he also controls more than 50 international patents on gear design, gear process, tools and machinery.